

UDK: 666.3.019; 622.785; 546.284

Synthesis and Sintering Impact on the Properties of Willemite Based Glass-Ceramics Using Rice Husk Waste as Silica Source

R. A. A. Wahab^{1,2*}, M. H. M. Zaid^{1*}, K. A. Matori¹, M. K. Halimah¹, H. A. A. Sidek¹, Y. W. Fen¹, A. Abdu³, M. F. M. Shofri¹, S. H. Jaafar¹

¹Department of Physics, Faculty of Science, Universiti Putra Malaysia, 43400 UPM Serdang, Selangor, Malaysia

²Faculty of Applied Sciences, University Teknologi MARA, Perak Branch Tapah Campus, 35400 Tapah Road, Perak, Malaysia

³Department of Forest Management, Faculty of Forestry, Universiti Putra Malaysia, 43400 UPM Serdang, Selangor, Malaysia.

Abstract:

The impact of sintering duration on willemite-based glass-ceramics (WGC) derived from the $ZnO-B_2O_3-SiO_2$ host system through a conventional melt-quenching method by incorporating rice husk ash (RHA) as the silica (SiO_2) source was comprehensively studied by means of physical, structural, and optical properties. The increment of sintering duration elevated the diffusivity rate resulting in a gradual increment of bulk density and linear shrinkage over sintering time. The XRD patterns affirmed the $\beta-Zn_2SiO_4$ phase formed after sintering at $700^\circ C$ for 2 h, followed by $\alpha-Zn_2SiO_4$ crystallization at a higher holding time. FESEM observation revealed that Zn_2SiO_4 embedded in the glassy solid phase and grew in equiaxed shape crystals as the holding time increased. Absorption spectra revealed the increasing trend in absorption bands with an increase in sintering duration due to the intensification of Zn_2SiO_4 crystallization thus escalating the green emission. Thus, this WGC will be applied as optically phosphor materials.

Keywords: Glass-ceramics; Sintering; Zinc silicate; Phase transformation; Photoluminescence.

1. Introduction

Synthetic zinc silicate (Zn_2SiO_4) phosphor has been artificially fabricated for over 100 years since it was first found due to its fluorescent characteristics under the ultraviolet ray [1]. It often appeared in yellow emission ($\beta-Zn_2SiO_4$) [2] but may probably appear in green ($\alpha-Zn_2SiO_4$) [3] and red ($\gamma-Zn_2SiO_4$) [4] due to its different crystallographic character. Thus, the fabrication of synthetic crystalline Zn_2SiO_4 has enormously contributed to the invention of willemite-based glass-ceramic as potent phosphor materials [5-7]. $\alpha-Zn_2SiO_4$ with polymorph of zinc orthosilicate as the most commonly found crystalline phase in Zn_2SiO_4 glass-ceramics. Significant attention has been put on the fabrication of Zn_2SiO_4 as it offers excellent glass transparency [8] and substantial fluorescence characteristics [9]. Optically, its wide bandgap has made it attentively produced as light-emitting diodes [7], laser diodes [10], display panel [11], and cathode-ray phosphor [12].

*) Corresponding author: rabiatul6341@perak.uitm.edu.my; mhmzaid@upm.edu.my

The innovation in fabricating Zn_2SiO_4 by incorporating silica (SiO_2) waste-based precursors has moved to another level. The increasing attention paid to the transfiguration makes Zn_2SiO_4 becoming more environmentally friendly, and also the cost of precursors has declined tremendously as pure SiO_2 is quite pricey [13]. Rice husk ash (RHA) was a favorable candidate as it was highly abundant along the years and contained higher SiO_2 content compared to the other SiO_2 waste-based materials such as soda-lime-silica (SLS) glass [14], palm kernel ash (PKA) [15] and coconut husk ash (CHA) [16]. To date, the incorporation of RHA in synthesizing phosphor materials has been successfully generated red [17], green, and blue [18] emissions, which is beneficial for producing white solid-state light materials. RHA was globally renowned for its reputable pollution resource. Thus, the production of Zn_2SiO_4 based glass-ceramic (WGC) by using the RHA will lead to a safer and pollution-free environment.

In recent years, there has been an increase in the number of literatures done in procuring WGC through solid-state sintering [19,20]. When compared to the chemical process and sol-gel technique, a substantial number of researches focused on the fabrication of WGC with the reinforcement of SiO_2 waste-based materials. The work done by Anuar et al. has highlighted the effect of sintering temperature on the structural and optical properties of ZnO-CHA [21]. The solid-state sintering process has considerably provided an alternative route not only due to its cost efficiency and simplicity in preparing the precursors, but also offers a significant improvement in physical, mechanical, and optical properties by merely adjusting the sintering environment [22]. Though sintering time does not play an essential role as sintering temperature, yet it can provide significant clarification through the studied properties.

Hence, the focus of this work is to study the effect of sintering time on the fabrication of WGC in the ZnO- B_2O_3 -RHA glass host system. The transformation of willemite crystals has been thoroughly investigated through densification changes, linear shrinkage, phase transformation, and optical luminescence. The optimization of the sintering environment may provide comprehensive findings in preparing potential solid-state lighting materials from waste materials at low temperatures to achieve high energy efficiency. Succinctly, this work will impart a remarkable finding in stipulating an alternative route of synthesizing willemite-based glass-ceramic from rice husk ash that can potentially become a green solid-state lighting material.

2. Materials and Experimental Procedures

2.1 Silica (SiO_2) extraction

In this experiment, double stage combustion (DSC) process was implemented to acquire SiO_2 from raw rice husk (RRH). Rice husk ash (RHA) was obtained after the RRH went through the DSC process. Initially, the RRH was collected from a rice company, BERNAS; located in Kuala Selangor, Malaysia. RRH went through a thorough cleaning process under tap water and distilled water until it was free of mud, dirt, and impurities. Afterward, the drying process took place in an oven overnight at $120^\circ C$. DSC process has been briefly explained [23], and the same method was implemented in this work. Eventually, fine RHA proceeded with structural analysis for further usage.

2.2 Preparation and characterization of starting materials

High purity zinc oxide, ZnO and boron oxide, B_2O_3 together with rice husk ash, RHA has incorporated together as precursors in preparing a series of ZnO- B_2O_3 - SiO_2 precursor glass with a composition weight of 65ZnO-15 B_2O_3 -20RHA. In this work, both ZnO (99.9 % purity) and B_2O_3 (99.9 %) were acquired from Sigma Aldrich, St. Louis, MO, USA. 40 g of

the composite was conventionally treated by a melt-quench process at 1350°C for 2 h before being poured down into the tap water bath set at room temperature for the quenching step. The glass frits formed afterward were then left dry overnight in an ambient condition. Later, it was crushed and ground into fine particles and sieved using an industrial sieve at < 45 μm. Next, 1g ground glass was pressed at 4.5 tons using a hydraulic pressing machine to form compacted disc shape green bodies with fairly ~13 mm in diameter and thickness of ~3 mm, and then subjected to a sintering process at 700°C in an electrical furnace at a heating rate of 10 °C/min for 2, 4 and 10 h. The sintered samples later were crushed, ground, and sieved to be characterized for physical, microstructural, and optical characteristics. A brief explanation regarding the flow chart of the method is shown in Fig. 1.

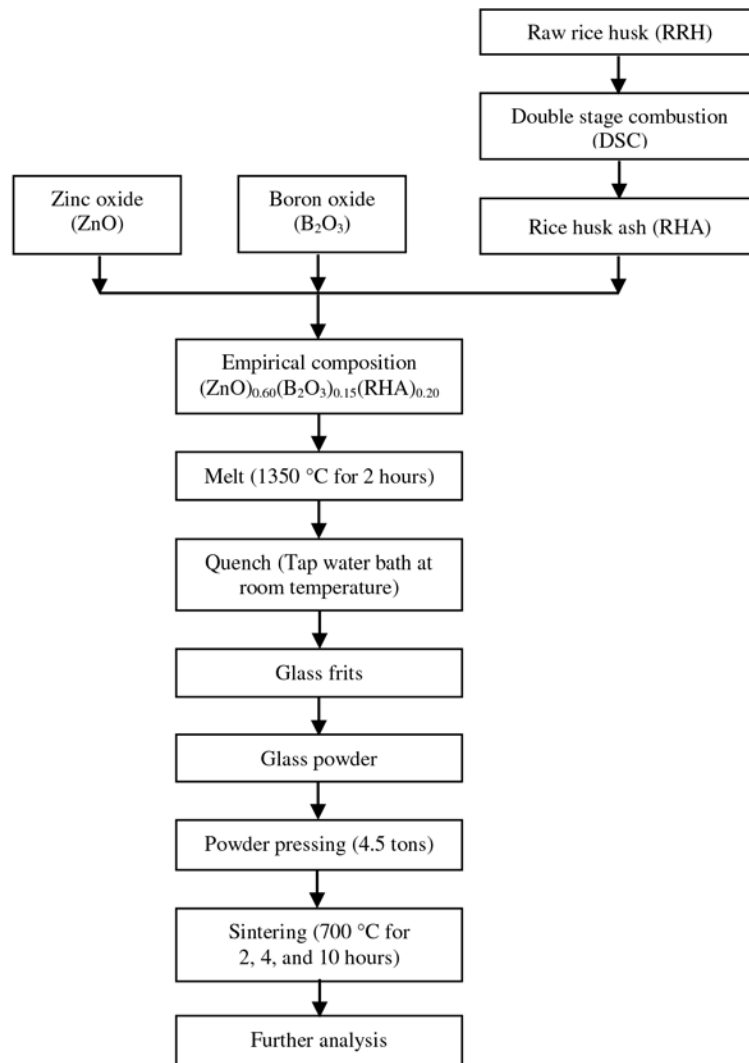


Fig. 1. Conventional process of melting, quenching, and sintering in procuring phosphor WGC.

The density measurement was obtained using a densimeter (MD-300S, Metler Toledo, FL, USA) in the immersion of distilled water at room temperature. In the case of bulk density, Archimedes' Principle was applied and expressed by the following formula:

$$\rho_{GC} = \frac{W_{air}}{W_{air} - W_{water}} \times \rho_{water} \quad (1)$$

where ρ_{GC} is the density of glass-ceramics (GC) samples, W_{air} is the weight of GC in air, W_{water} is the weight of distilled water, and ρ_{water} is the density of distilled water. Meanwhile, the linear shrinkage measurement was taken according to the geometrical changes of the sintered GC by using a digital vernier caliper (150 mm, MITUTOYO, Japan).

The structural identification was confirmed using the X-ray diffraction (XRD) (Philips, PW3040/60 model) at 20-80° in the range of 2θ . Whereas, the inspection of the existing functional groups in the RHA and GC samples was carried out on the Fourier Transform Infrared (FTIR) spectroscopy (Perkin Elmer, Spectrum 100 model) by applying attenuated total reflection (ATR) method. The optical absorption spectra of glass and glass-ceramic samples were identified using a UV-Visible spectrophotometer (Shimadzu, UV-3600 model) and the emission intensity of luminescence spectra have been measured using a photoluminescence spectrometer (Perkin Elmer, LS 55 model) and AS ONE handy UV lamp.

3. Results and Discussion

The primary purpose of Double Stage Combustion (DSC) was to environmentally convert the raw rice husk (RRH) in brown color into rice husk ash (RHA) in white color such in Fig. 2. The same figure, it also shows the FTIR spectrum of RHA. The white RHA in powder form was examined under the influence of reflectance infrared (IR) spectra of wavenumbers in the range of 400-1400 cm^{-1} . The RHA generated three prominent bands located at 452, 498, and 1082 cm^{-1} . The lower wavenumber is showed a stronger band where 452 cm^{-1} corresponded to stretching and bending vibration of O-Si-O [24] and 498 cm^{-1} corresponded to Si-O-Si bending vibration bond [25], compared to a hump presented at a higher wavenumber, while 1082 cm^{-1} corresponded to Si-O-Si asymmetric stretching vibration [26]. The presence of SiO_2 in the FTIR spectrum can be corroborated by the data from XRD spectroscopy that has been recently published, thus representing the diffraction pattern that can show the amorphous or crystalline nature of the analyzed sample. The reported pattern shows the consistency of a single major peak identified at $2\theta = 22^\circ$ with a small-scale shoulder that can be attributed to amorphous SiO_2 [27-28].

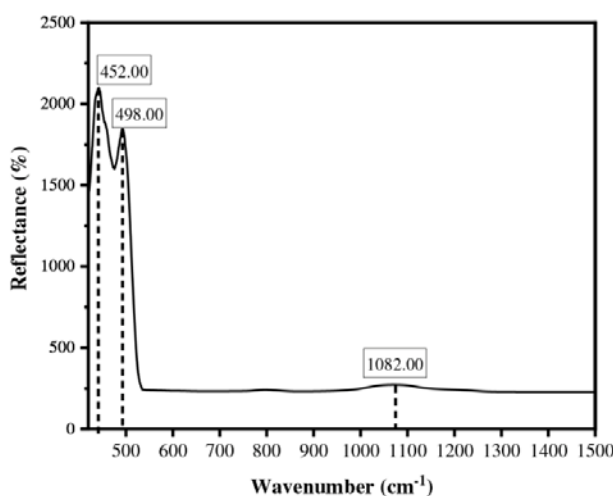


Fig. 2. FTIR absorbance spectra of heat-treated rice husk ash (RHA).

Physical properties of the glass-ceramics have been investigated through bulk density accompanied by linear shrinkage as a function of sintering time was illustrated in Fig. 3. below. These methods are an effective way to comparatively review the compactness of the studied materials together with their geometrical changes [29]. The sintering process is one of the fundamental elements in powder metallurgy. It is before facilitating powder compaction alongside powder densification whilst crystallization is happening. The figure shows the pattern of bulk density and linear shrinkage of the compacted glass sintered at 700°C holds for 2, 4, and 10 h have been increased respectively [30]. The increment was due to the compaction structurally in the sintered samples. This pattern significantly represents the actual behavior of atomic diffusion, where the diffusivity was proportionally increased to the temperature applied. The sufficient energy supplied, causing the grain boundaries diffusion happened between the host particles. The willemite crystal growth has coarsened the grains thus eliminating voids located inter-grains and increasing the compacted pattern of the atomic structures [31]. This was also related to the intensification of willemite as sintering time increased, the density increased due to the shortening bond length by forming ZnO_4 octahedral groups [14].

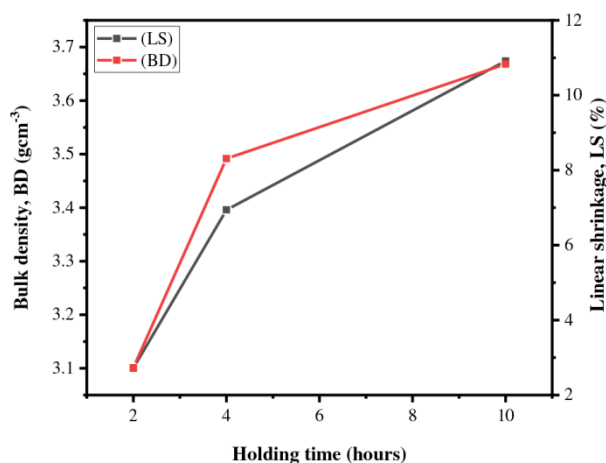


Fig. 3. Bulk density and linear shrinkage of the compacted glass sintered at 700°C with different durations.

The structural characteristics of the ternary $ZnO-B_2O_3-SiO_2$ precursor glass and glass-ceramics concerning the sintering time variation were characterized through XRD measurement and shown in Fig. 4. The as-quench glass (refer as 0 h) shows an apparent diffuse band at around $2\theta = 30^\circ$ with no sharp peaks was structurally found in amorphous glass nature due to the long-range disordered structure [32]. The progression of sintering time depicted an intensified diffraction peak belongs to $\alpha-Zn_2SiO_4$ and $\beta-Zn_2SiO_4$. This demonstrated the intensity of ions diffusing into the sample was increased at a longer duration sintering process. Hereafter, the crystal growth rate was enhanced, and the greater size of crystals developed in the sample. $\beta-Zn_2SiO_4$ phase appeared after sintered at 700°C for 2 h duration. A similar pattern was obtained for the glass-ceramic sample sintered at 700°C for 4 h. Interestingly, the XRD pattern change occurred due to the phase transformation of the $\alpha-Zn_2SiO_4$ phase when sintered for 10 h.

The XRD diffraction peak of the glass and glass-ceramic samples sintered for more extended periods indexed and it resembled the same pattern compared to the $\beta-Zn_2SiO_4$ phase with JCPDS file No. 19-1479 and also zinc orthosilicate, $\alpha-Zn_2SiO_4$ phase (JCPDS file No. 37-1485). Also, it had been found that the improvement of the sintering period up to 10 hours, led to the progress of diffraction peak intensity of the crystal phase [8]. This finding can be

corroborated by the values for full width at half maxima (FWHM) obtained from the X'pert highscore software was found to be decreased with the progression of the sintering duration from 0.5196, 0.2273, and 0.1624, respectively.

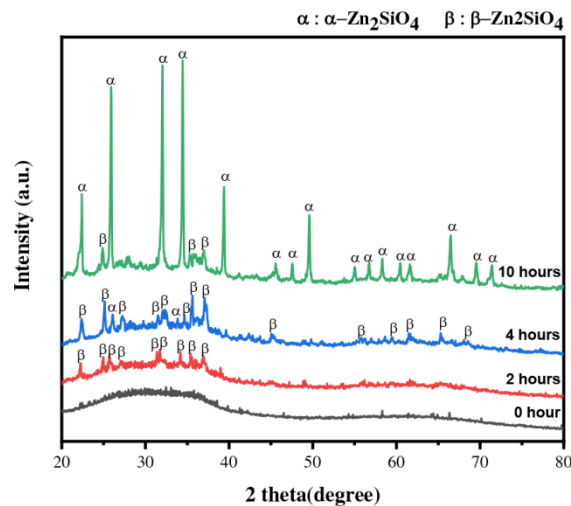


Fig. 4. The XRD pattern of the WGC sintered at 700°C for a different duration.

The morphological changes of the WGC sintered with different sintering times are shown in Fig. 5. It can be seen that the sintering process dramatically influenced surface morphology. Willemite crystal has appeared as early at sintering time of 2 h in equiaxed-granular form. Entirely only, higher duration of the sintering process occurs, more compact the structure and grain sizes were generated and consequently lower the glassy surface of the final product. Increment of holding sintering time densified the β - Zn_2SiO_4 crystal particles that were grown relatively uniform into equiaxed α - Zn_2SiO_4 supported [21].

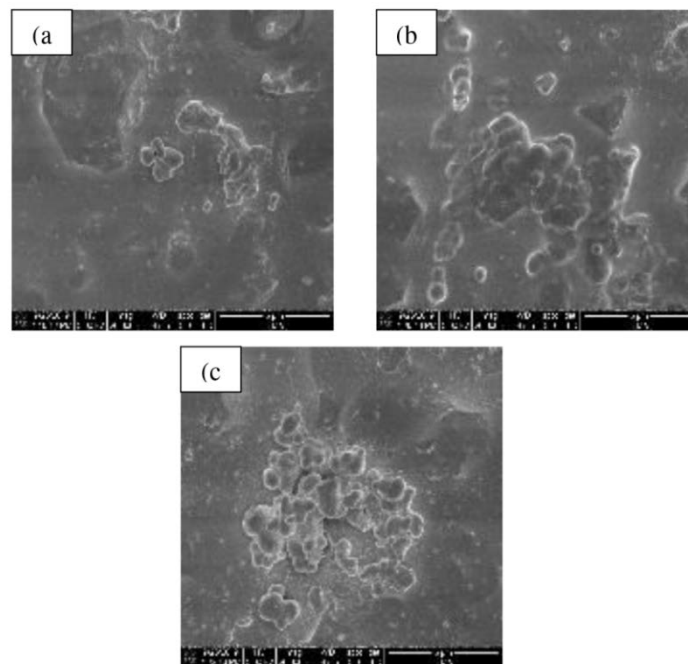


Fig. 5. Structural morphology of samples sintered at 700°C for (a) 2 h, (b) 4 h, and (c) 10 h.

The optical absorbance spectra performed in the ultraviolet wavelength range 200 - 800 nm were meant to provide important information regarding the electronic band structures in materials either in bulk or powder form is presented in Fig. 6. The absorption spectra of the samples sintered at 700°C for different duration were recorded at room temperature. The absorption edges for each sintered sample clearly show sharp decrement along the absorption spectra indicates its crystalline state. The uplifted patterns of the sintered samples and the increases of sintering temperature and holding time are due to the increment of Zn_2SiO_4 crystallinity which acts as light scattering centers in the glass, thus increasing the absorption rate. This uplifting of the absorption curve results from the light scattering phenomenon of Zn_2SiO_4 crystal [33]. Typically, the scattering effect is even more detected in the sample treated for 10 h because an extra quantity of greater Zn_2SiO_4 crystals size in the glass-ceramic sample was treated for a higher duration. The observed transition at 360 nm notified as to the peak energy. The samples exposed no significant evolution along with the absorbance with the sintering behaviors duration which kept the absorption values over the visible region in the spectrum range.

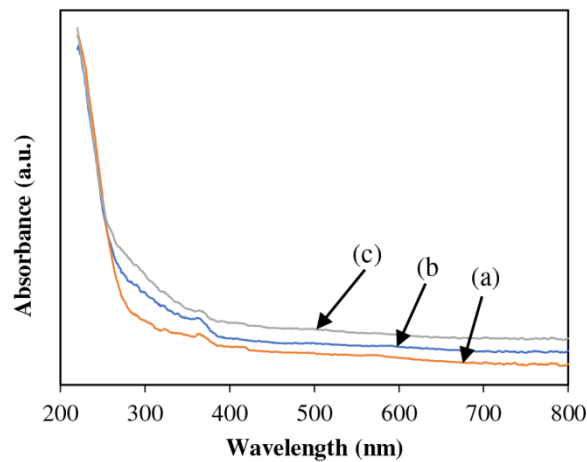


Fig. 6. UV-vis spectra of WGC sintered at 700°C for (a) 2 h, (b) 4 h, and (c) 10 h.

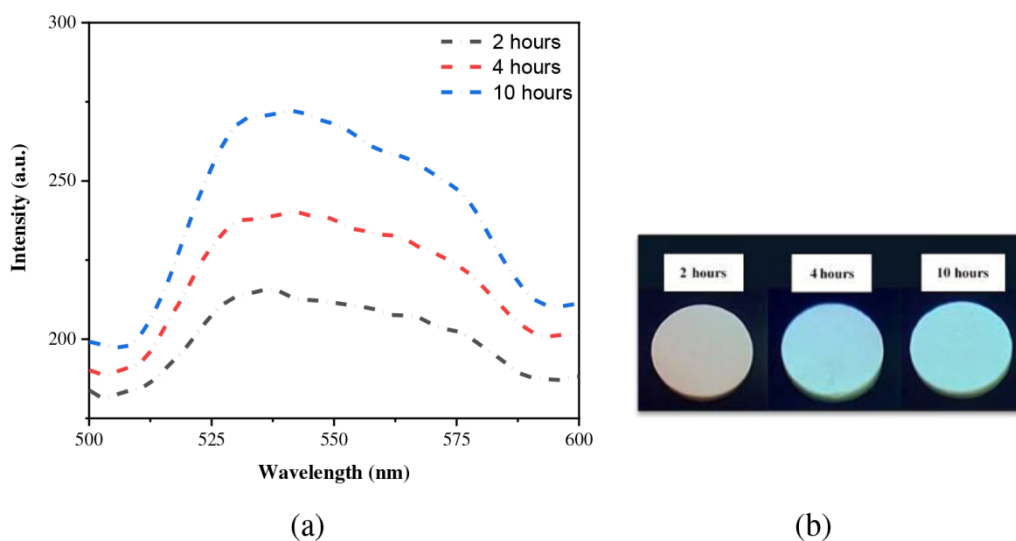


Fig. 7. Emission spectra of WGC samples sintered for the different duration (a) excited at 360 nm under the photoluminescence spectrometer and (b) excited at 254 nm under UV lamp.

The photoluminescence spectra of the WGC were shown in Fig. 7. The embedded Zn_2SiO_4 crystals were proven to exhibit strong emission of green luminescence at 530 nm after being excited at a wavelength of 360 nm meanwhile the bulk WGC samples are radiated under direct UV rays excited at 254 nm. The emission intensified along with the longer holding time due to improvement in crystallinity. As elaborated in Fig. 4, the crystallization of willemite intensified when the sintering time increased, resulting in a long order network disruption and weakening of the borate network as zinc ions were much bigger than boron ions and [34]. Thus, this projected the decrement of non-bridging oxygen (NBO) in the WGC where willemite crystal is always regarded as the UV emission source. Comparing the strongly bonded oxygen (BO), the NBO contained a weakly bonded electron made it easily excited.

4. Conclusion

In this recent study, zinc silicate glass-ceramics (WGC) were successfully prepared using conventional melt-quench of $\text{ZnO-B}_2\text{O}_3\text{-RHA}$ ternary glass system. Physical characteristics were analyzed in the form of bulk density and linear shrinkage. Whereas the phase transformation characteristics of zinc silicate glass-ceramics were described using XRD and FESEM observation. The optical characteristics were well explained by PL and UV-Vis spectroscopy techniques. The bulk density and linear shrinkage increased respectively due to the increment in the crystallinity of the Zn_2SiO_4 crystal phase inside the sintered samples. The XRD showed the minimum temperature introduced in this study to crystallize zinc silicate was at 700°C prior to the metastable of $\beta\text{-Zn}_2\text{SiO}_4$ crystal phase, which later transformed and crystallized into a stable state $\alpha\text{-Zn}_2\text{SiO}_4$ phase in irregular size of the equiaxed form. The obtained emission band was attributed to green emission, which intensified as the duration increased.

Acknowledgments

This research was supported by the Ministry of Education (MOE) through the Fundamental Research Grant Scheme (FRGS/1/2019/STG07/UPM/02/3). The authors gratefully acknowledge the financial support for this study from the Malaysian Ministry of Education (MOE) and the laboratory facilities provided by the Faculty of Science, University Putra Malaysia (UPM), Materials Synthesis and Characterization Laboratory, Institute of Advanced Technology, University Putra Malaysia (UPM), and Faculty of Applied Science, University Teknologi MARA (UiTM), Perak Branch Tapah Campus.

5. References

1. M. T. Tsai, Y. H. Lin, & J. R. Yang, Characterization of manganese-doped willemite green phosphor gel powders, in IOP Conference Series: Materials Science and Engineering, 18 (2011) 032026.
2. R. Ye, G. Jia, D. Deng, Y. Hua, Z. Cui, S. Zhao, L. Huang, H. Wang, C. Li, & S. Xu, Controllable synthesis and tunable colors of $\alpha\text{-}$ And $\beta\text{-Zn}_2\text{SiO}_4\text{:Mn}^{2+}$ nanocrystals for UV and blue chip excited white LEDs, Journal of Physical Chemistry C, 115 (2011) 10851-10858.
3. V. Sivakumar, A. Lakshmanan, S. Kalpana, R. S. Rani, R. S. Kumar, & M. T. Jose, Low-temperature synthesis of $\text{Zn}_2\text{SiO}_4\text{:Mn}$ green photoluminescence phosphor Low-

- temperature synthesis of Zn_2SiO_4 : Mn green photoluminescence phosphor, *Journal of Luminescence*, 132 (2012) 1917-1920.
4. S. S. A. Rashid, S. H. A. Aziz, K. A. Matori, M. H. M. Zaid, and N. Mohamed, Comprehensive study on effect of sintering temperature on the physical, structural and optical properties of Er^{3+} doped ZnO-GSLS glasses, *Results in Physics*, 7 (2017) 2224-2231.
 5. A. Tarafder, A. R. Molla, S. Mukhopadhyay, & B. Karmakar, Fabrication and enhanced photoluminescence properties of Sm^{3+} -doped ZnO– Al_2O_3 – B_2O_3 – SiO_2 glass derived willemite glass-ceramic nanocomposites, *Optical Materials*, 36 (2014) 1463-1470.
 6. M. H. M. Zaid, K. A. Matori, H. J. Quah, W. F. Lim, H. A. A. Sidek, M. K. Halimah, W. M. M. Yunus, & Z. A. Wahab, Investigation on structural and optical properties of SLS-ZnO glasses prepared using a conventional melt quenching technique, *Journal of Materials Science: Materials in Electronics*, 26 (2015) 3722-3729.
 7. S. A. A. Wahab, K. A. Matori, H. A. A. Sidek, M. H. M. Zaid, M. M. A Kechik, A. Z. K. Azman, R. E. M. Khaidir, M. Z. A. Khiri, & N. Effendy, Synthesis of cobalt oxide Co_3O_4 doped zinc silicate based glass-ceramic derived for LED applications, *Optik*, 179 (2018) 919-926.
 8. M. F. S. M. Shofri, M. H. M. Zaid, K. A. Matori, Y. W. Fen, Y. Yaakob, S. H. Jaafar, S. A. A. Wahab, & Y. Iwamoto, Phase Transformation, Optical and Emission Performance of Zinc Silicate Glass-Ceramics Phosphor Derived from the ZnO– B_2O_3 –SLS Glass System, *Applied Sciences*, 10 (2020) 4940.
 9. I. A. Auwalu, U. H. Jamo, D. G. Diso, A. F. Inuwa, A. Aminu, M Alhassan, & S. A. Umar, Effect of Bi^{3+} on Metallization and Polarizability Properties on Willemite Glass Ceramics from Waste Materials, *Dutse Journal of Pure and Applied Sciences*, 4 (2018) 360-369.
 10. S. A. M. Abdel-Hameed & F. H. Margha, Preparation, crystallization and photoluminescence properties of un-doped nano willemite glass ceramics with high ZnO additions, *Optik*, 206 (2020) 164374.
 11. A. Morell & N. El Khiati, Green Phosphors for Large Plasma TV Screens, *Journal of The Electrochemical Society*, 140 (2022) 2019-2022.
 12. L. Xiong, K. Saito, S. Wada, & E. H. Sekiya, Utilization of Rice Husk to Synthesize High-Performance Phosphors, 19 (2009) 39-43.
 13. M. H. M. Zaid, K. A. Matori, H. A. A. Sidek, M. K. Halimah, Z. Wahab, Y. W. Fen, & I. Alibe, Synthesis and characterization of low cost willemite based glass–ceramic for opto-electronic applications, *Journal of Materials Science: Materials in Electronics*, 27 (2016) 11158–11167.
 14. M. H. M. Zaid, S. H. A. Aziz, M. K. Halimah, W. M. M. Yunus, Z. A. Wahab, & N. Samsudin, Fabrication and Crystallization of ZnO-SLS Glass Derived Willemite Glass-Ceramics as a Potential Material for Optics Applications, *Journal of Spectroscopy*, 2016 (2016) 1-7.
 15. P. E. Imoisili, K. O. Ukoba, & T. C. Jen, Green technology extraction and characterisation of silica nanoparticles from palm kernel shell ash via sol-gel, *Journal of Materials Research and Technology*, 9 (2020) 307-313.
 16. M. F. Anuar, Y. W. Fen, M. H. M. Zaid, N. A. S. Omar, & R. E. M. Khaidir, Sintering temperature effect on structural and optical properties of heat treated coconut husk ash derived SiO_2 mixed with ZnO nanoparticles, *Materials*, 13 (11) (2020) 2555.
 17. R. E. M. Khaidir, Y. W. Fen, M. H. M. Zaid, K. A. Matori, N. A. S. Omar, M. F. Anuar, S. A. A. Wahab, & A. Z. K. Azman, Optical band gap and photoluminescence studies of Eu^{3+} -doped zinc silicate derived from waste rice husks, *Optik*, 182 (2018) 486-495.

18. I. M. Alibe, K. A. Matori, H. A. A. Sidek, Y. Yaakob, U. Rashid, A. M. Alibe, M. H. M. Zaid, & M. Z. A. Khiri, Effects of Calcination Holding Time on Properties of Wide Band Gap Willemite Semiconductor Nanoparticles by the Polymer Thermal Treatment Method, *Molecules*, 23 (2018) 873.
19. E. A. G. Engku Ali, K. A. Matori, E. Saion, S. H. A. Aziz, M. H. M. Zaid, & I. M. Alibe, Effect of sintering temperatures on structural and optical properties of ZnO-Zn₂SiO₄ composite prepared by using amorphous SiO₂ nanoparticles, *Journal of the Australian Ceramic Society*, 55 (2018) 115-122.
20. M. F. S. M. Shofri, M. H. M. Zaid, R. A. A. Wahab, K. A. Matori, S. Hj. A. Aziz, & Y. W. Fen, The effect of boron substitution on the glass-forming ability, phase transformation and optical performance of zinc-boro-soda-lime-silicate glasses, *Journal of Materials Research and Technology*, 9 (2020) 6987-6993.
21. M. F. Anuar, Y. W. Fen, M. H. M. Zaid, & N. A. S. Omar, Optical studies of crystalline ZnO-SiO₂ developed from pyrolysis of coconut husk, *Materials Research Express*, 7 (2020) 1-9.
22. S. H. Jaafar *et al.*, Effect of sintering temperatures and foaming agent content to the physical and structural properties of wollastonite based foam glass-ceramics, *Science of Sintering*, 52 (2020) 269-281.
23. R. A. Abdul Wahab, M. H. Mohd Zaid, S. Hj. A. Aziz, K. Amin Matori, Y. W. Fen, & Y. Yaakob, Effects of Sintering Temperature Variation on Synthesis of Glass-Ceramic Phosphor Using Rice Husk Ash as Silica Source, *Materials*, 13 (2020) 5413.
24. R. A. Bakar, R. Yahya, & S. N. Gan, Production of High Purity Amorphous Silica from Rice Husk, *Procedia Chemistry*, 19 (2016) 189-195.
25. M. A. Rida and F. Harb, Synthesis and Characterization of Amorphous Silica Nanoparticles from Aqueous Silicates Using Cationic Surfactants, *Journal of Metals, Materials and Minerals*, 24 (2014) 37-42.
26. D. An, Y. Guo, Y. Zhu, & Z. Wang, A green route to preparation of silica powders with rice husk ash and waste gas, *Chemical Engineering Journal*, 162 (2010) 509-514.
27. A. G. N. D. Darsanasiri, F. Matalkah, S. Ramli, K. Al-Jalode, A. Balachandra, & P. Soroushian, Ternary alkali aluminosilicate cement based on rice husk ash, slag and coal fly ash, *Journal of Building Engineering*, 19 (2018) 36-41.
28. L. A. Quintero Sierra & D. M. Escobar Sierra, Synthesis and Bioactivity Evaluation of a Rice Husk-Derived Bioactive Glass," *Materials in Nanomedicine and Bioengineering*, 71 (2019) 302-307.
29. M. K. Halimah, M. N. Ami Hazlin, & F. D. Muhammad, Experimental and theoretical approach on the optical properties of zinc borotellurite glass doped with dysprosium oxide, *Spectrochimica Acta - Part A: Molecular and Biomolecular Spectroscopy*, 195 (2018) 128-135.
30. N. Quratul, A. Ismail, K. Sa'at, M. Hafiz, & M. Zaid, Effect of Sintering Time on Microstructure and Electrical Properties of Varistor Ceramics ZnO-CoO-SLS Glass, *Science of Sintering*, 53 (2021) 509-518.
31. E. Montoya-Quesada, M. A. Villaquirán-Caicedo, R. Mejía de Gutiérrez, & J. Muñoz-Saldaña, Effect of ZnO content on the physical, mechanical and chemical properties of glass-ceramics in the CaO-SiO₂-Al₂O₃ system, *Ceramics International*, 46 (2020) 4322-4328.
32. N. A. S. Omar, Y. W. Fen, K. A. Matori, M. H. M. Zaid, & N. F. Samsudin, Structural and optical properties of Eu³⁺ activated low cost zinc soda lime silica glasses, *Results in Physics*, 6 (2016) 640-644.
33. A. Tarafder, A. R. Molla, C. Dey, & B. Karmakar, Thermal, structural, and enhanced photoluminescence properties of Eu³⁺-doped transparent willemite glass-ceramic nanocomposites, *Journal of the American Ceramic Society*, 96 (2013) 2424-2431.

34. G. Borodi, L. C. Bolundut, & P. Pascuta, Effect of erbium(III) oxide addition on thermal properties and crystallization behavior of some zinc-borate glasses, AIP Conference Proceedings, 1917 (2017) 040004.

Сажетак: Утицај дужине синтеровања је праћен кроз физичка, структурна и оптичка својства стакло керамике на бази вилемита (WGC) добијеног из $ZnO-B_2O_3-SiO_2$ система кроз конвенционални метод топљење-квенчинг инкорпорацијом пепела као извора силицијума (SiO_2). Продужено време синтеровања утиче на пораст брзине дифузије што даље резултује градијентном повећању густине узорака и линеарном скупљању. XRD је указао на фазу $\beta-Zn_2SiO_4$ која се формира након синтеровања на $700^\circ C$ током 2 сата, што је праћено кристализацијом $\alpha-Zn_2SiO_4$ са дужином задржавањем. FESEM је показао да је Zn_2SiO_4 уграђен у чврсту стакласту фазу и да расте у еквиаксијалне кристале са дужином задржавања. Абсорпциони спектри су показали тренд раста абсорпционих трака са продужетком синтеровања услед кристализације Zn_2SiO_4 која утиче на зелену емисију. Према томе, WGC ће бити употребљен као оптички фосфоран материјал.

Кључне речи: стакло-керамика, синтеровање, цинк силикат, фазна трансформација, фотолуминесценција.

© 2022 Authors. Published by association for ETRAN Society. This article is an open access article distributed under the terms and conditions of the Creative Commons — Attribution 4.0 International license (<https://creativecommons.org/licenses/by/4.0/>).

